Nucleation rate of kink-antikink pairs in a driven and overdamped deformable chain

David Yemélé and Timoléon C. Kofané
Laboratoire de Mécanique, Faculté des Sciences, Université de Yaoundé I, Boîte Postale 812, Yaoundé, Cameroun
(Received 4 December 1995; revised manuscript received 16 September 1996)

The equilibrium nucleation rate of thermally activated kink-antikink pairs, in nonlinear deformable substrate potential systems coupled to an external applied field, is determined analytically at low temperature, and in the limit of strong damping. We focus our attention on a class of parametrized one-site potential $V_{\mathrm{RP}}(u,r)$ whose shape can be varied as a function of parameter r and which has the sine-Gordon shape as the particular case. We derive the driven kink velocity as well as the average velocity of the displacement of a particle as a function of an applied field. We show that for a given temperature this average velocity not only depends on the external field, but also on the shape parameter r. The model is used to describe the diffusion of atoms on metallic surfaces. Numerical values are estimated for the diffusion of hydrogen in tungsten (W) and ruthenium (Ru) substrates. [S1063-651X(97)16505-9]

PACS number(s): 41.20.Jb

I. INTRODUCTION

A great deal of attention has been devoted to the study of large amplitude excitations like soliton, kink, and other solitary-wave motions in one dimensional systems. Dislocation kinetics have been modeled by solitary waves [1,2] in the past. The Frenkel-Kontorova model of dislocation is a well-known example. Progress has been made in the development of well defined kink mechanics. Typically, the continuum approximation is invoked to reduce the N-body problem resulting from the lattice dynamics of the kinks. Also, statistical mechanics of kinks has been studied. In recent years, it has found new interest, unrelated to previous results in the theory of kinks in dislocations. This development was stimulated by an application of the transfer-operator technique to systems exhibiting solitons [3].

The related problem of the study of the soliton becomes more difficult when the existence of perturbations is taken into account, because their inclusion into nonlinear lattice problems always leads to nonlinear intractable partial differential equations. These perturbations currently encountered in a wide variety of systems in physics, chemistry, and biology [4,5] are from various sources: dissipations, impurities, external fields, and thermal fluctuations (noise). Using various techniques [6–9], many studies have been carried out to analyze their effects on the structural and dynamical behavior of solitons [9–11]. In general, there appears a modulation of parameters such as velocity, mobility, soliton extension, and amplitude. On the other hand, other studies based on different approaches [12–14] have focused on kink-antikink pair formation. Their nucleation rate, as well as the average displacement velocity of a particle of the system, has also been discussed. In this case, the presence of the soliton in the system can be appreciated as a result of thermal fluctuations favored by the applied field. One can make a further distinction between geometrical and thermal kinks. As a major distinction we recall that the latter ones are always produced in pairs and their density strongly depends on the temperature [14].

The first approach developed by Guyer and Miller [13] is based on a transfer-operator technique [15] combined with the Bogoliubov-Born-Green-Kirkwood-Yvon hierarchy approximation. It has been shown that this method yields correct results in the high-temperature regime.

The second approach developed by Büttiker and Landauer [14] is based on nucleation theory [16–18]. It is valid at low temperatures and strong coupling between adjacent particles. A great feature of this approach lies in the fact that its answers are closely related to concepts already developed in the dislocation literature. Following this approach, Büttiker and Landauer [14] have presented a detailed calculation of the nucleation rate of thermal kink-antikink pairs in the overdamped sine-Gordon (SG) chain.

These results concerning the SG chain are very encouraging, but they remain, nevertheless, limited in their applicability to real physical systems. In those systems, the shape of the nonlinear one-site potential may deviate considerably from that attributed to the local potential. To ameliorate the understanding of the nonlinear excitations in real materials and model field theories, few deformable models have appeared in the literature, such as parametrized double-well potentials [19–26], where the choice of one or the other model depends on the physical system under consideration. For example, in the hydrogen-bonded system, the large displacement of heavy ions can significantly modify the barrier height of the double-well potential associated with the light protons [27]. Also deformable SG models have been proposed [28–31]. The H/W adsystem (hydrogen atoms adsorbed on a tungsten surface) is a well-known example [32]. The thermodynamical properties [33] as well as the chaotic behavior [34,35] of deformable nonlinear systems have been studied. Therefore, the study of the nucleation rate of kink-antikink pairs with a nonlinear periodic substrate potential $V_{RP}(u,r)$, whose shape can be varied continuously as a function of the parameter r and which has the SG shape as a particular case [28], becomes interesting. We assume that the coupling between adjacent particles is strong so that neighboring particles remain close to each other. Similarly, we confine our attention in the limit of strong damping and low temperature $\Delta E_N \gg k_B T$, where ΔE_N is the nucleus energy, k_B is the Boltzmann constant, and T is the temperature. For this purpose, we use the nucleation theory of Büttiker and

Landauer on this model to evaluate the nucleation rate.

The paper is organized as follows. In Sec. II, we present the model and the resulting overdamped equation of motion of the field displacement. In Sec. III, we study the critical nucleus and derive the nucleation rate of kink-antikink pairs. The average velocity of the displacement field of a particle as well as the velocity of the driven kink are presented in Sec. IV. We point out in Sec. V that the model described above (see Sec. II) is a convenient one, well describing a real adsystem situation. Experimental values of the lattice parameters for H/W and H/Ru adsystems are used to estimate the average velocity of hydrogen atom at a surface diffusion of adsorbates induced by the electrical field. Finally, we make concluding remarks in Sec. VI.

II. MODEL DESCRIPTION

The model under consideration consists of a chain of interacting particles of mass m, equally spaced by the lattice constant a. These particles are coupled to each other via the nearest-neighbor interaction energy $V_c(\phi_{i+1}-\phi_i)$, and are placed in an underlying nonlinear periodic substrate potential $V_{\mathrm{RP}}[(2\pi/a)\phi_i,r]$ with amplitude ε_s, so that the Hamiltonian for the model is

$$H=\sum_i \left\{\frac{1}{2}\,m\dot{\phi}_i^2+V_c(\phi_{i+1}-\phi_i)+\varepsilon_s V_{\mathrm{RP}}[(2\pi/a)\phi_i,r]\right\}, \tag{2.1}$$

where ϕ_i is the longitudinal displacement of the ith particle from their equilibrium position along the x axis, and the overdot is the time derivative.

It is often convenient to describe the nearest-neighbor interaction with the Morse potential

$$V_c(\phi_{i+1}-\phi_i)=D_s\{\exp[-b(\phi_{i+1}-\phi_i)]-1\}^2, \tag{2.2}$$

where D_s is the energy of the interaction of the particle occupying the nearest sites and b, characterizing the anharmonicity of the potential, is defined as $b=1/a$.

In the strong coupling limit (displacive regime), ϕ_{i+1} and ϕ_i are sufficiently close together, so that (i) $V_c(\phi_{i+1}-\phi_i)$ can be approximated by a second-order Taylor expansion about zero, (ii) $(\phi_{i+1}-\phi_i)=a(\partial\phi/\partial x)$. Hence, the Hamiltonian (2.1) can be replaced by a continuum representation

$$H=\int \frac{dx}{a}\left\{\frac{1}{2}\,m\left(\frac{\partial\phi}{\partial t}\right)^2+\frac{2V_c''(0)}{2}\left(\frac{\partial\phi}{\partial x}\right)^2+\varepsilon_s V_{\mathrm{RP}}[(2\pi/a)\phi,r]\right\}. \tag{2.3}$$

For the sake of convenience, we use the dimensionless displacement field $u(x,t)=(2\pi/a)\phi(x,t)$. Thus Eq. (2.3) becomes

$$H=\int dx\left\{\frac{1}{2}\,M\left(\frac{\partial u}{\partial t}\right)^2+\frac{k}{2}\left(\frac{\partial u}{\partial x}\right)^2+V_0V_{\mathrm{RP}}(u,r)\right\}, \tag{2.4}$$

where the parameters M, k, and $\mathbf{V}_0$ have the dimensions of (mass)$\times$(length), (energy)$\times$(length), and (energy)$\times$(length)$^{-1}$, respectively, and are defined as

$$M=ma/(4\pi)^2,\quad k\equiv 2V_c''(0)a^3/(4\pi)^2=D_sa/(2\pi)^2,$$
$$V_0=\varepsilon_s/a. \tag{2.5}$$

The dynamical behavior of a particle of a chain (in the case of the conservative system) is a solution of the Euler-Lagrange equation following from Eq. (2.4):

$$M\left(\frac{\partial^2u}{\partial t^2}\right)-k\left(\frac{\partial^2u}{\partial x^2}\right)+V_0dV_{\mathrm{RP}}(u,r)/du=0. \tag{2.6}$$

We focus our attention on the substrate potential $V_{\mathrm{RP}}(u,r)$ introduced by Remoissenet and Peyrard [28]

$$V_{\mathrm{RP}}(u,r)=(1-r)^2\,\frac{(1-\cos u)}{1+r^2+2r\cos u},\qquad |r|<1 \tag{2.7}$$

with constant amplitude and variable shape. Then, Eq. (2.6) exhibits static kink solutions given implicitly by (see [28,29])

$$\frac{x}{d'}=\mathrm{sgn}(\pi-u)\left\{(1-\beta^2)^{1/2}\tanh^{-1}\left[\frac{(1-\beta^2)}{1+\beta^2\tan^2(u/2)}\right]^{1/2}-\tanh^{-1}\left[\frac{1}{1+\beta^2\tan^2(u/2)}\right]^{1/2}\right\} \tag{2.8a}$$

for $0\leqslant r<1$ and

$$\frac{x}{d''}=\mathrm{sgn}(u-\pi)\left\{[(1-\beta^2)^{1/2}/\beta]\tan^{-1}\left[\frac{(1-\beta^2)}{\beta^2+\tan^2(u/2)}\right]^{1/2}+\tanh^{-1}\left[\frac{\beta^2}{\beta^2+\tan^2(u/2)}\right]^{1/2}\right\} \tag{2.8b}$$

for $-1<r\leqslant 0$ with

$$d'=\xi_0/\beta,\quad d''=\xi_0\beta \tag{2.9}$$

$$\xi_0=(k/V_0)^{1/2}, \tag{2.10}$$

and

$$\beta=\frac{1-|r|}{1+|r|}. \tag{2.11}$$

The terms d' and d'' have the dimensions of length and give a measure of the pseudokink width for $r\geqslant 0$ and $r\leqslant 0$, respectively. The antikink solutions are obtained by replacing u by $2\pi-u$ in Eqs. (2.8). It can be shown that the energies of these static kinks (2.8) (and antikinks) are [29]

$$E_s=8\beta(kV_0)^{1/2}(1-\beta^2)^{-1/2}\tanh^{-1}(1-\beta^2)^{1/2},\quad r\geqslant 0 \tag{2.12a}$$

$$E_s=8(kV_0)^{1/2}(1-\beta^2)^{-1/2}\tan^{-1}[(1-\beta^2)^{1/2}/\beta],\quad r\leqslant 0. \tag{2.12b}$$

Since we deal with a dissipative and driven chain, we add a dissipative force $M\gamma_0\partial u/\partial t$, the applied field f, and the

fluctuating thermal force $R(x,t)$ in Eq. (2.6), so that the equation of motion of a particle of the chain becomes

$$M\left(\frac{\partial^2 u}{\partial t^2}\right)+\gamma\left(\frac{\partial u}{\partial t}\right)-k\left(\frac{\partial^2 u}{\partial x^2}\right)+dV(u,r,F)/du=R(x,t), \tag{2.13}$$

where γ_0 is the damping constant and connected to γ by

$$\gamma=M\gamma_0. \tag{2.14}$$

The fluctuating forces describe the coupling of the chain to a heat bath and verify the following correlation function:

$$\langle R(x,t)\rangle=0,$$

$$\langle R(x,t)R(x',t')\rangle=2k_BT\gamma\delta(x-x')\delta(t-t'). \tag{2.15}$$

The term $V(u,r,F)$ defined as

$$V(u,r,F)=V_0V_{\mathrm{RP}}(u,r)-Fu \tag{2.16}$$

is the resulting one-site potential, in the external field f. It is easy to show that f and F are related by

$$F=f/2\pi. \tag{2.17}$$

The applied field f may be due to mechanical stress or to an electrical field if we are in the presence of charged particles. In this later case, the field f and the electrical field E_e are related through the equation

$$f=e^*E_e, \tag{2.18}$$

where e^* is the coupling constant or the effective charge of each particle.

When the field is applied, the minimum ($u_{sn}=2n\pi$, where n is an integer number) of the potential $V_{\mathrm{RP}}(u,r)$ will be raised with respect to the adjacent potential maximum $[u_{in}=(2n+1)\pi]$, while the adjacent potential well will be lowered. These minima and maxima of the potential, which are known as Peierls valleys and Peierls hills, respectively, will be shifted and eventually disappear when the field F approaches $F_m(r)$ defined as

$$F_m/V_0=\frac{2\sqrt{2}\beta^2[(3\beta^2-1)+\sqrt{\Delta}]\sqrt{\sqrt{\Delta}-3(1-\beta^2)}}{(5\beta^2-3+\sqrt{\Delta})}, \tag{2.19a}$$

with

$$\Delta=9\beta^4-14\beta^2+9. \tag{2.19b}$$

The Peierls valleys u_{sn} and Peierls hills u_{in} admit for small values of F and/or r the following expressions:

$$u_{sn}=\arcsin\,\theta+2n\pi, \tag{2.20a}$$

$$u_{in}=\arcsin\,\theta+2(n+1)\pi, \tag{2.20b}$$

with

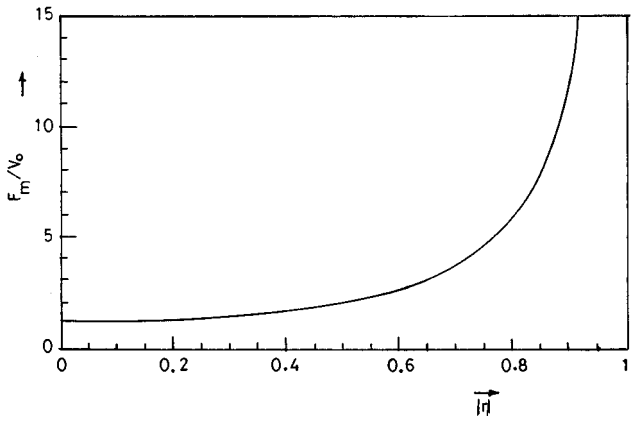

FIG. 1. Plot of the maximum value of the field F (in dimensionless unit F/V_0) for which the Peierls valleys exist as a function of the shape parameter r.

$$\theta=\frac{4r(F/V_0)}{(1+r^2)G}\sqrt{1-(F/V_0)^2}+(F/V_0)\left[1-\left(\frac{4r(F/V_0)}{(1+r^2)G}\right)^2\right]^{1/2}, \tag{2.20c}$$

$$G=\left[\left(\frac{1-r^2}{1+r^2}\right)^4+\left(\frac{4r(F/V_0)}{(1+r^2)}\right)^2\right]^{1/2}. \tag{2.20d}$$

For large field F (but less than F_m), those Peierls valleys and hills can be evaluated numerically, see Fig. 1.

Since we are dealing with an overdamped chain, we will mostly focus on the limit of high damping, such that the inertial term in Eq. (2.13) can be neglected compared to the frictional one. Hence, Eq. (2.13) becomes

$$\gamma\left(\frac{\partial u}{\partial t}\right)-k\left(\frac{\partial^2 u}{\partial x^2}\right)+dV(u,r,F)/du=R(x,t) \tag{2.21}$$

and the energy functional of the system is now, from the Hamiltonian (2.4),

$$E(u)=\int dx\left\{\frac{1}{2}k\left(\frac{\partial u}{\partial x}\right)^2+V(u,r,F)\right\}. \tag{2.22}$$

This energy (2.22) will play an important role in Sec. III when evaluating the number of kink-antikink pairs in the deformable model.

III. NUCLEATION RATE OF KINK-ANTIKINK PAIRS

It is straightforward to show that the variation of the energy of the chain between two adjacent Peierls valleys (u_{sn} and u_{sn+1}) due to the application of the field F, evaluated from the energy functional (2.22), is $2\pi Fl$, where l is the chain length. The state u_{sn} is metastable *vis a vis* of the state u_{sn+1}. Thus the segment of the chain which was initially at the state of higher energy u_{sn} is likely to jump to the next state with lower energy u_{sn+1} triggered off by stochastic forces $R(x,t)$. This segment of the chain with lower energy is connected to the segment in the Peierls valley with higher energy through kink-antikink pairs (the nucleus). The transition described above would be possible only if the fluctuations produce within the system a minimum of the energy $\Delta E_N \gg k_BT$ necessary to create a critical nucleus (u_N). More

precisely, if the transferred section is too small, then the attraction between the newly formed kink and antikink predominates the driven field F and the incipient nucleus collapses, leading to the restoration of the initial state (u_{sn}). If, however, the transferred section is long enough, the driven field predominates and the kink-antikink pair expands. Thus the transferred section of the chain grows. There is a critical nucleus which is the configuration relevant to the saddle point of the surface energy. Then, in this section, we study this configuration (i.e., the energy ΔE_N which has to be surmonted) and its stability, and derive the number of kink-antikink pairs per unit length and time.

The critical nucleus is a local extremum of the surface energy. Hence, it is a stationary solution ($\partial u/\partial t=0$) of Eq. (2.21). Setting $\Delta u=u_N-u_s$, the first integration of the resulting equation yields

$$\frac{1}{2}\,\xi^2\left(\frac{d\Delta u}{dx}\right)^2=(1+2\varepsilon\,\cos u_s)\left\{\frac{1-\cos\,\Delta u\left[1+\dfrac{2\varepsilon\Delta u\,\tan u_s}{1+2\varepsilon\,\cos u_s}\right]+\left[1+\dfrac{2\varepsilon\Delta u\,\tan u_s}{1+2\varepsilon\,\cos u_s}\right]\tan u_s\,\sin\Delta u}{1+2\varepsilon\,\cos u_s(\cos\Delta u-\tan u_s\,\sin\Delta u)}\right.$$

$$\left.-\frac{\Delta u\,\tan u_s/(1+2\varepsilon\,\cos u_s)}{1+2\varepsilon\,\cos u_s(\cos\Delta u-\tan u_s\,\sin\Delta u)}\right\},\qquad(3.1)$$

where

$$\varepsilon=r/(1+r^2)\qquad(3.2)$$

and

$$\xi^2=\xi_0^2\left(\frac{1+r^2}{1-r^2}\right)^2\left\{\frac{(1+2\varepsilon\,\cos u_s)^3}{\cos u_s+2\varepsilon(1+\sin^2 u_s)}\right\},\qquad(3.3)$$

with energy

$$\Delta E_N=\int dx\left[k\left(\frac{du}{dx}\right)^2\right].\qquad(3.4)$$

Equation (3.1) describes the configuration that starts from the stationary state u_s with a decreasing length ξ which depends on r and F. For $F=0$, this length tends to $\xi_0\beta$ for $r>0$, ξ_0/β for $r<0$ and ξ_0 for $r=0$ (SG case), where β is given by Eq. (2.11). By setting $r=0(\varepsilon=0)$, Eq. (3.1) leads to the SG one [14]

$$(1/2)\xi^2\left(\frac{d\Delta u}{dx}\right)^2=1-\cos\,\Delta u+(\sin\,\Delta u-\Delta u)\tan u_s.\qquad(3.5)$$

The first obvious remark is that Eq. (3.1) is analytically untractable. However, on the basis of physical considerations an approximate expression could be derived. For instance, in the absence of the applied field ($F=0$), Eq. (3.1) yields the stationary equation derived from Eq. (2.13). Hence, in this case, the solution of Eq. (3.1) is a kink [Eqs. (2.8)] and an antikink infinitely apart. Now, in order to derive an expression of Δu for small fields, we observe that (Fig. 2) the amplitude of the critical nucleus is close to 2π and its form is that of a kink and an antikink separated by a distance δ_c. It is, therefore, natural to assume for such a solution an analytical expression for a kink given by Eq. (2.8), and an antikink separated by the critical distance

$$\delta_c=-\beta\xi_0\,\ln[(4\pi F/V_0)/\beta]\quad\text{for}\quad 0\leqslant r<1,\qquad(3.6a)$$

$$\delta_c=-(1/\beta)\xi_0\,\ln[(4\pi F/V_0)\beta]\quad\text{for}\quad -1<r\leqslant 0,\qquad(3.6b)$$

which is determined by the flat-top of the solution $u_N(x)$. The amplitude Δu_m of this nucleus can be found by substituting Δu into Eq. (3.1) by $(2\pi-\theta)$ where θ is a small quantity. Following this treatment, we obtain

$$\Delta u_m=2\pi-(4\pi F/V_0)^{1/2}/\beta\quad\text{for}\quad 0\leqslant r<1\qquad(3.7a)$$

and

$$\Delta u_m=2\pi-\beta(4\pi F/V_0)^{1/2}\quad\text{for}\quad -1<r\leqslant 0.\qquad(3.7b)$$

The energy (ΔE_N) of this configuration is evaluated as follows: in the absence of the applied field, the activation energy of kink-antikink pairs tends to the sum of the rest energy of a kink and an antikink; i.e., $2E_s$, where E_s is given by Eq. (2.12). Now, if the chain is submitted to a small field,

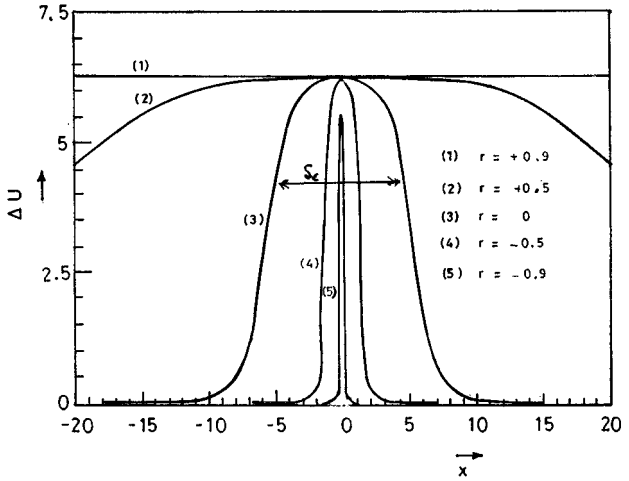

FIG. 2. Critical nucleus for a low field $F/V_0=10^{-4}$ with the width δ_c [Eq. (3.8)] for a few r. δ_c decreases rapidly when r increases and tends to zero when r approaches 1.

we have to incorporate the energy gained by the system or to calculate the energy changes associated with small changes in the configuration. Assuming that the energy is stationary at $u_N(x)$ with respect to small changes in this configuration, the variation of the energy is to first order in dF. Hence, from Eq. (2.22) we have

$$d(\Delta E_N) = -dF \int \Delta u_N(x)dx. \tag{3.8}$$

Using the fact that, the largest part of the critical nucleus is the flat-top (Fig. 2) whose width is given by Eqs. (3.6), one obtains

$$d(\Delta E_N) = -2\pi\delta_c dF\,. \tag{3.9}$$

Integration of Eq. (3.9) yields

$$\Delta E_N = 2E_s\{1+F\beta(2\pi\xi_0/E_s)\ln[(4\pi F/V_0)^{1/2}/(\beta e)]\}$$

$$\text{for } 0\leqslant r<1, \tag{3.10a}$$

$$\Delta E_N = 2E_s\{1+(F/\beta)(2\pi\xi_0/E_s)\ln[\beta(4\pi F/V_0)^{1/2}/e]\}$$

$$\text{for } -1<r\leqslant 0. \tag{3.10b}$$

For values of F close to $F_m(r)$ and for r close to zero, the amplitude Δu_m tends to zero. The critical nucleus corresponds to a small amplitude nucleus (SAN). The right-hand side of Eq. (3.1) can be accurately approximated by a third-order Taylor expansion about zero. The integration of the resulting equation yields

$$\Delta u_{\rm SAN} = \Delta u_m \ \mathrm{sech}^2(x/2\xi), \tag{3.11a}$$

with

$$\Delta u_m = 3\left(\frac{1+r^2}{1-r^2}\right)^2 \tan u_s\left[\frac{1-2\varepsilon\ \cos u_s+4\varepsilon/\cos u_s}{1-5\varepsilon\ \cos u_s}\right]. \tag{3.11b}$$

Inserting Eq. (3.11a) into Eq. (3.4), we obtain the energy of the small amplitude nucleus

$$\Delta E_{\rm SAN} = (24/5)(kV_0)^{1/2}(\Delta u_m)^2\left(\frac{1+r^2}{1-r^2}\right)(F/V_0)^{1/2}\left\{1/\tan u_s + 4\varepsilon(1+2\varepsilon\ \cos u_s)(F/V_0)\left(\frac{1+r^2}{1-r^2}\right)^2\right\}^2. \tag{3.12}$$

In order to evaluate ΔE_N for all values of $F<F_m$, we have integrated numerically Eq. (3.4) together with Eq. (3.1). The results are plotted in Fig. 3. We note that two facts can contribute to lowering the nucleus energy in this model: First, an increase of the applied field, such as a SG chain, and second, a potential with a sufficiently flat bottom ($r\to 1$). If the first case corresponds, in the fact, to lower the nucleus amplitude, the second, however, corresponds to a very large nucleus. Since ΔE_N corresponds to the energy of creation of a critical nucleus, this result suggests that, physically, the critical nucleus would be more easily created in systems which can be modeled by the potential with a flat bottom.

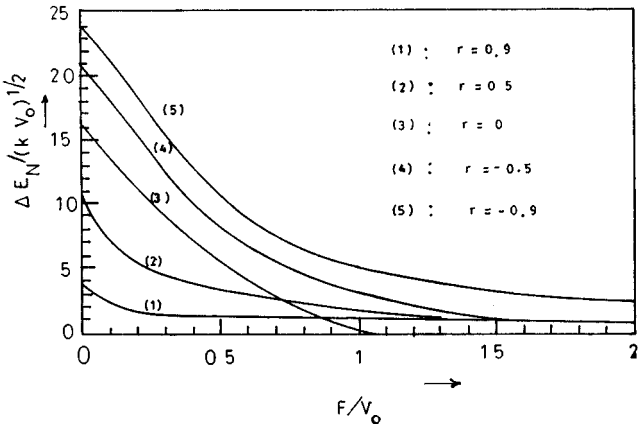

FIG. 3. Activation energy barrier for the nucleation of kink-antikink pairs vs the field F/V_0 for different values of r. The curves are independent of the chain characteristics.

Let us turn our attention now to an examination of the stability of the critical nucleus. To test this stability, we add a small perturbation $\delta u(x,t)$ [which can be assumed to have the form $\delta u(x,t)=\delta u_\lambda(x)\exp(-\lambda t)$] to $u_N(x)$ in an equation derived from an energy functional, that is, Eq. (2.9) [$\delta E/\delta u = -\gamma(\partial u/\partial t)$]. After linearization with respect to δu, this leads to the formal Schrödinger eigenvalues equation

$$L(u_N(x))\delta u_\lambda(x) = (\lambda/\Gamma)\,\delta u_\lambda(x), \tag{3.13}$$

where $L(u_N(x))$ is the linear operator given by

$$L(u_N(x)) = -\xi^2\frac{d^2}{dx^2} + v(u_N(x)), \tag{3.14}$$

with the scattering potential

$$v(u_N(x)) = [d^2V(u_N,r,F)/du^2]/[d^2V(u_S,r,F)/du^2] \tag{3.15}$$

and

$$\Gamma = (V_0/\gamma)d^2V(u_s,r,F)/du^2, \tag{3.16}$$

where

$$d^2V(u_s,r,F)/du^2 = (1-r^2)^2 \times\frac{(1+r^2)\cos u_s - 2r\ \cos^2 u_s + 4r}{(1+r^2+2r\ \cos u_s)^3}. \tag{3.17}$$

Equation (3.16) reduces to $\Gamma=(V_0/\gamma)\cos u_s$ for $r=0$ (the SG case).

The energy of this state (i.e., the configuration near the saddle) is given by

$$E[u_N(x)+\delta u(x,t)] = E(u_N) + (a\gamma/2)\sum_n\ \lambda_n^N\eta_n^2, \tag{3.18}$$

which is to second order of the perturbation $\delta u(x,t)$, evaluated from the energy functional (2.22).

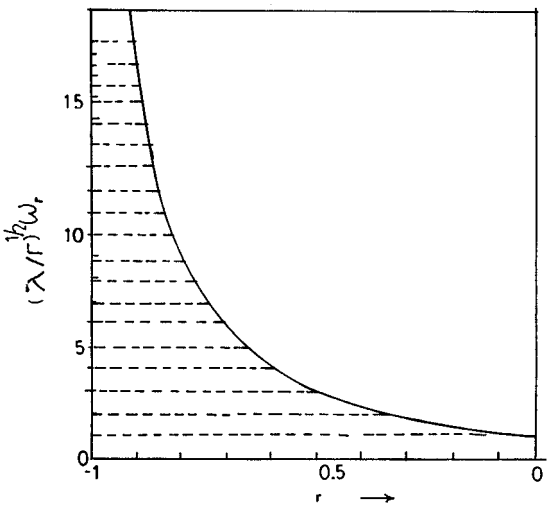

FIG. 4. Localized modes of the system's excitation spectrum in the presence of the kink ($F=0$) (dashed curve). The full curve represents $\omega_r=(1-r)/(1+r)$.

In the absence of the applied field ($F=0$), the system excitation spectrum obtained by integrating Eq. (3.13) is that of two kinks infinitely apart. We note that when $r\geqslant 0$ the system possesses one bound state with an eigenvalue $\lambda_n=0$ corresponding to the Goldstone mode. Moreover, when r decreases from 0 to -1, internal modes appear, for instance, for $r=-0.5$, the spectrum possesses exactly four bound states whereas for $r=-0.9$, the number of bound states is 20 (Figs. 4 and 5). No unstable mode ($\lambda_n<0$) has been found.

In the presence of the field F, one notes the positive eigenvalues and a negative eigenvalue (λ_0^N) corresponding to the stable and unstable modes, respectively. The presence of the unstable mode ($\lambda_0^N<0$) results from the application of the field F. This mode is of great importance in the formation of kink-antikink pairs. In fact, from Eq. (3.18), one can make some remarks. In the presence of perturbations, the energy near the saddle increases in the direction of all stable eigenmodes ($\lambda_n^N>0$) and remains constant in the direction of the Goldstone mode while it decreases in the direction of the unstable mode. If the amplitude of this mode η_0 is negative, we assume that the contraction of the critical nucleus leads to restoration of the initial state u_s. When this amplitude is positive, the critical nucleus expands leading to the formation of an independent pair of a kink and an antikink.

We now look at the number of kink-antikink pairs created per unit time and length using the approach of Brinkman [16], Landauer and Swansom [17], and Langer [18], (the BLSL approach) (see Ref. [14]). We start with the Fokker-Planck equation derived from Eqs. (2.15) and (2.21)

$$\frac{\partial P}{\partial t}+\int\left(\frac{dx}{a}\right)\left(\frac{\delta j(u(x))}{\delta u(x)}\right)=0, \tag{3.19}$$

with

$$j(u)=-\left(\frac{1}{\gamma a}\right)\left[\frac{\delta E}{\delta u}P+k_BT\left(\frac{\delta P}{\delta u}\right)\right], \tag{3.20}$$

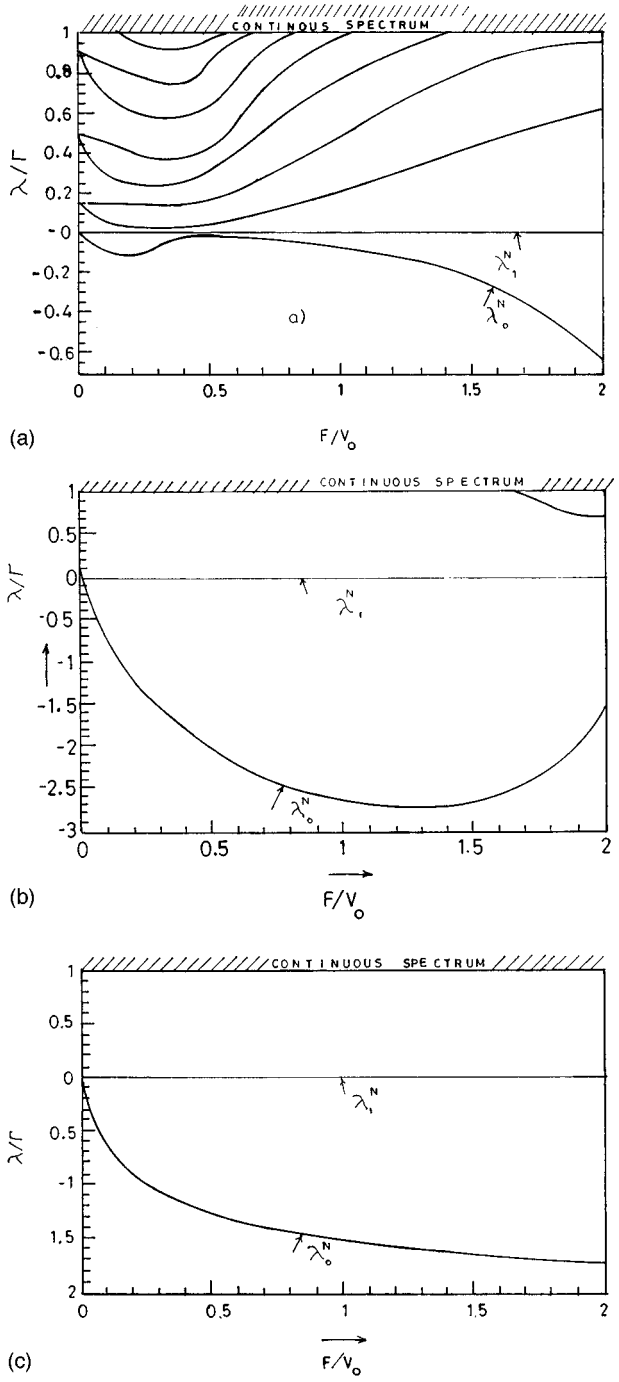

FIG. 5. Eigenvalues of the perturbations of the critical nucleus as a function of F/V_0 for (a) $r=-0.5$, (b) $r=0.5$, and (c) $r=0.9$.

where $j(u)$ and $P(u)$ denote the current and distribution probability, respectively. The equilibrium probability distribution at the state u_N is

$$P(u_N)=P_0\exp(-E(u_N)/k_BT), \tag{3.21}$$

where P_0 is the normalization factor.

The BLSL approach consists of a correction factor $g(u)$ to the local equilibrium distribution probability

$$P(u)=g(u)\exp(-E(u)/k_BT). \tag{3.22}$$

Substituting Eq. (3.22) into Eq. (3.20) one obtains

$$j(u)=-(k_BT/\gamma a)\left(\frac{\delta g}{\delta u}\right)\exp[-E(u)/k_BT]. \quad (3.23)$$

Near the saddle, this expression can be rewritten as

$$j_n(\{\eta\})=-(k_BT/\gamma a)\left(\frac{\delta g}{\delta \eta_n}\right)\exp\left[-\left(E(u_N)+(a\gamma/2)\sum_n \lambda_n^N\eta_n^2\right)\Big/ k_BT\right], \quad (3.24)$$

where we have used the quadratic approximation for the energy $E(u+\delta u)$. In the steady state, the calculation of the number of kink-antikink pairs per unit time and length j_N is similar to that performed by Büttiker and Landauer [14]. Using the same approach, Eq. (3.24) yields

$$j_N=\left(\frac{\Gamma}{2\pi}\right)^{3/2}(\gamma/k)^{1/2}(|\lambda_0^N|/\Gamma)^{1/2}\prod_{n>1}^{p-1}\times(\Gamma/\lambda_n^N)^{1/2}(\Delta E_N/k_BT)^{1/2}(Q)\exp(-\Delta E_N/k_BT), \quad (3.25)$$

where j_N is the nucleation rate, λ_n^N is the eigenvalue of the nonuniform state, p the number of bound states of the operator $L(u(x))$ and Q the product of the eigenvalues of the nonlocalized eigenmodes of the critical nucleus. Using Bohr and Sommerfeld's approximation quantization rule [14,36], we obtain

$$\ln(Q^2)=\int_1^{+\infty}(\rho_s-\rho_N)\ln(\lambda/\Gamma)d(\lambda/\Gamma), \quad (3.26)$$

where ρ_s and ρ_N are the density of state of the uniform state u_s and nonuniform state u_N, respectively, given by

$$\rho_s=(1/2\pi\xi)\int_{-\infty}^{+\infty}dx[1/(\lambda/\Gamma-1)^{1/2}] \quad (3.27a)$$

and

$$\rho_N=(1/2\pi\xi)\int_{-\infty}^{+\infty}dx\{1/[\lambda/\Gamma-\nu(u(x))]^{1/2}\}. \quad (3.27b)$$

The factor Q is a function of the applied field F and the shape parameter r. Its numerical evaluation is plotted in Fig. 6. From the spectrum of $L(u(x))$ and the factor Q, we are able to evaluate the nucleation rate of kink-antikink pairs j_N.

From Eqs. (3.25), one can make some comments: (i) The nucleation rate j_N of the kink-antikink pairs are temperature and deformable parameter dependent, (ii) their expression $[\sim T^{-1/2}\exp(-\Delta E_N/k_BT)]$ allows us to say that it is an increasing function of temperature, and (iii) due to mathematical difficulties, it is not possible to predict its behavior as a function of r, even if its numerical evaluation for a few values of r shows an increase with r. This numerical analysis will be checked indirectely from the average velocity of a particle in the chain which has the same behavior as j_N.

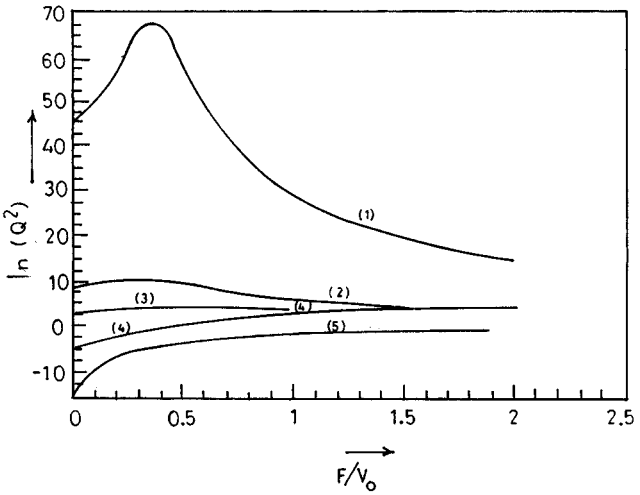

FIG. 6. Product of the eigenvalues of the state u_s divided by the product of the eigenvalues of the nonlocalized eigenvalues of the critical nucleus vs (F/V_0) for a few values of r.

In order to relate this result (j_N) to the physical parameter easily experimentally accessible, we will evaluate in Sec. IV the average displacement velocity of a particle in the chain. This question has been of interest in the theory of dislocation for more than three decades [37].

IV. AVERAGE DISPLACEMENT VELOCITY OF PARTICLES

At low temperatures and in the absence of fluctuations, the particles undergo small amplitude oscillations around their equilibrium position. In a macroscopic viewpoint, the system is at equilibrium. A remarkable displacement of particles comes from its transition from one site to an adjacent one, due to the passing of the soliton triggered by stochastic forces. The average velocity of this displacement $\langle \partial u/\partial t\rangle$ is thus determined by the number of kinks and antikinks passing the particle per unit time. Hence, this velocity is given by

$$\langle \partial u/\partial t\rangle = 2\pi(2v j_N)^{1/2}, \quad (4.1)$$

where v is the kink velocity. The solution sketched here established in the SG chain case is still valid, even in this model. Indeed, Eq. (4.1) has been obtained by the assumption that in the limit of heavy damping the kink-antikink collision is destructive. Now, the kinklike solution of the unperturbed equation (2.4) interacts strongly with the antikink (in the absence of perturbations) [29], and this interaction can lead to the total destruction of both kink and antikink or to the formation of the breather. Then, the presence of perturbations should contribute to intensify this interaction. Consequently, any collisions between a kink and an antikink in the limit of heavy damping is destructive.

Equation (4.1) shows that to find the average velocity of a particle of the chain, we have thus to find the kink velocity. To evaluate this velocity, we now investigate the transition connecting two minima $u_s(r,F)$ and $u_s(r,F)+2\pi$ of the potential $V(u,r,F)$ of the traveling-wave form $u(x+vt)$

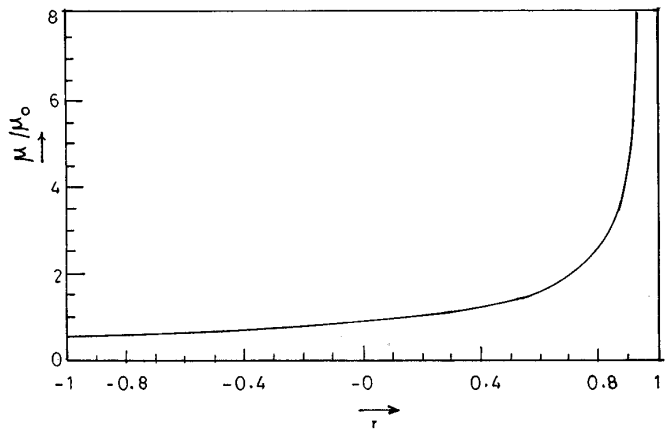

FIG. 7. The driven kink mobility in unit of $\mu_0=(k/V_0)^{1/2}/\gamma$ plotted as a function of the shape parameter r.

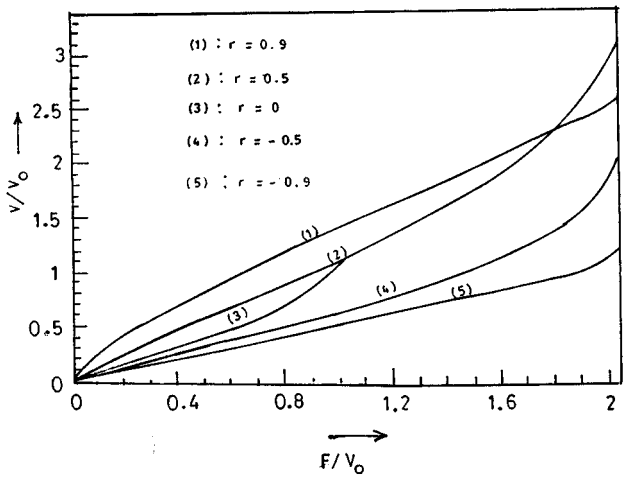

FIG. 8. Increase of the propagational velocity in unit of v_0 of the driven kink with increase of F/V_0 for different values of r.

$=u(z)$ of Eq. (2.1) in the absence of stochastic forces where v is the propagational velocity along x. $u(z)$ verifies the equation

$$k(d^2u/dz^2)-\gamma v(du/dz)-dV(u,r,F)/du=0. \quad (4.2)$$

In the absence of the external field F and damping, any solution of this equation can move with any constant velocity between zero and the sound velocity on the chain. However, in the driven and damped chain, the field F accelerates the initial motion of the kink which becomes uniform when the kink acquires a final velocity v determined by the balance between the total energy loss due to dissipation in the particle picture and the total work done by the external field. For small fields, the velocity is linear to F. In this case, the soliton mobility can be derived in a most simple manner by [38]

$$v/F\equiv\mu=2\pi k/(\gamma E_s), \quad (4.3)$$

where E_s is the kink rest energy given by Eqs. (3.10). The plot of $\mu(r)$is given in Fig. 7. The increase of r enhances the kink mobility. To make this physical behavior more clear, we find the velocity v in the whole range of F, we select the appropriated value of γv corresponding to the transition from one Peierls with zero initial velocity to an adjacent one with zero final velocity. The result for $v(r,F)$ is of the form [39]

$$v(r,F)=v_0 g(F/V_0,r), \quad (4.4)$$

where $v_0=(kV_0)^{1/2}/\gamma$ is a unit of velocity and the function g is defined by the curve plotted in Fig. 8. For small fields, g is linear in F and increases monotonically with an increasing field to a value $v^*=v_0 g^*$ at $F=F_m$. For example, for $r=-0.5$, $g^*=2.01$; for $r=0.5$, $g^*=3.2$; and $g^*=1.19$ for $r=0$ [14]. The stability of this driven kink has been well established [39].

We now have all the information necessary to calculate the velocity of particles in the chain in the presence of a field F. The results plotted in Figs. 9 and 10 in units of (V_0/γ) are based on a computational evaluation of Eqs. (3.25) and (4.1), and depend on reduced temperature $\tau=k_BT/(V_0k)^{1/2}$ and the shape parameter r. Figure 10 shows that the average velocity with which a particle advances is sensitive to r and as r increases $\langle\partial u/\partial t\rangle$ increases. It is, however, difficult to generalize this behavior for the mean velocity as a function of r because the results plotted in Fig. (10) refer to only a few values of r. But, it is physically possible to predict an increase in the mean velocity with r since, as shown in the preceding section, the total energy need to nucleate a kink-antikink pair decreases as r increases. Then, it would be easier to create a kink in the chain where the potential has a flat bottom $(r\rightarrow 1)$ than that where the potential has a flat-top $(r\rightarrow -1)$.

V. APPLICATION TO THE DIFFUSION OF HYDROGEN ATOMS ON METALLIC SURFACES

The model described in Sec. II has applications to the problem of surface diffusion of atoms and molecules adsorbed on metal surfaces. This problem is an odd one and still attracts the attention of many physicists since the results so far obtained are not satisfactory. This is due to the fact that there are many contradictions or gaps in existing measurements [40]. The research in the field has been carried out analytically and experimentally with computational methods.

Indeed, the model of Sec. II may be viewed as a one-dimensional chain of adatoms with a deformable potential $V_S(\phi,r)$. This potential is produced by the interaction of an adatom with substrate atoms, where the parameter r could account for the temperature dependance of the substrate or for the geometry of the surface of the metallic substrate. For instance, an estimate for the H/W adsystem yields $r\simeq -0.3$ [32]. Thus, we apply the results of the above analytical study to estimate the kink mobility and its diffusion constant (under the effects of thermal fluctuations); at last, the mean displacement velocity of a hydrogen atom on a Ru and W substrates induced by the applied electrical field E_e is investigated.

We assume that a unit cell contains only one adatom and that the lattice parameters (D, a, ε_s, and the damping coefficient γ_0) do not depend on the temperature or the external field. We focus our attention on two adsystems H/W and H/Ru, where available data exist. The diffusion of hydrogen atoms on various planes of W and Ru has been analyzed

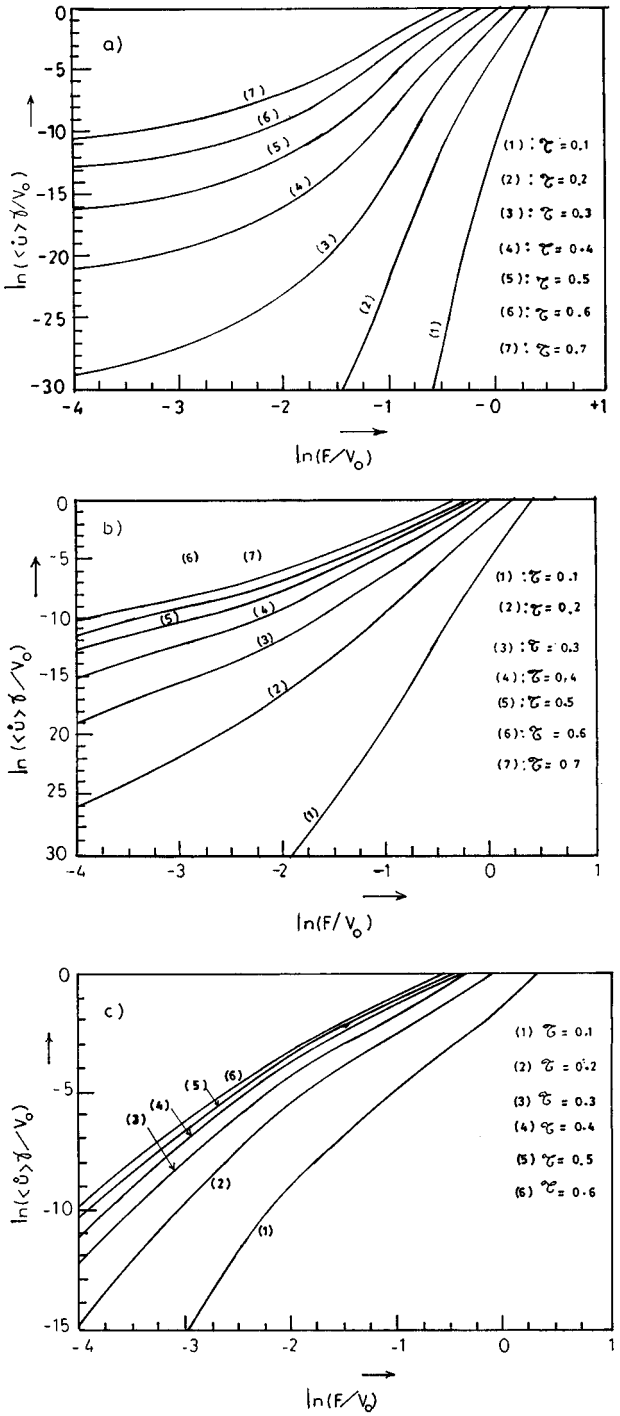

FIG. 9. Average velocity of particles $\langle \partial u/\partial t \rangle \equiv \langle \dot{u} \rangle$ in a dimensionless unit as a function of the applied field: for different temperature $\tau = k_B T/(kV_0)^{1/2}$ with (a) $r = -0.5$, (b) $r = 0.5$, and (c) $r = 0.9$.

using the field ion shadowing method [40,41] and the laser induced desorption-refilling method [40,42]. The measurements indicated that on these metallic substrates, the potential barrier ε_s varies between 0.10 and 0.50 eV. Also the coupling constant or effective charge e^* transferred when an atom is displaced from one equilibrium site to the next one generally differs from the charge of the adatom particle. In the case of the diffusion of hydrogen atoms, the measurements indicated that $e^* = 0.1e - 0.7e$, where e is the protonic

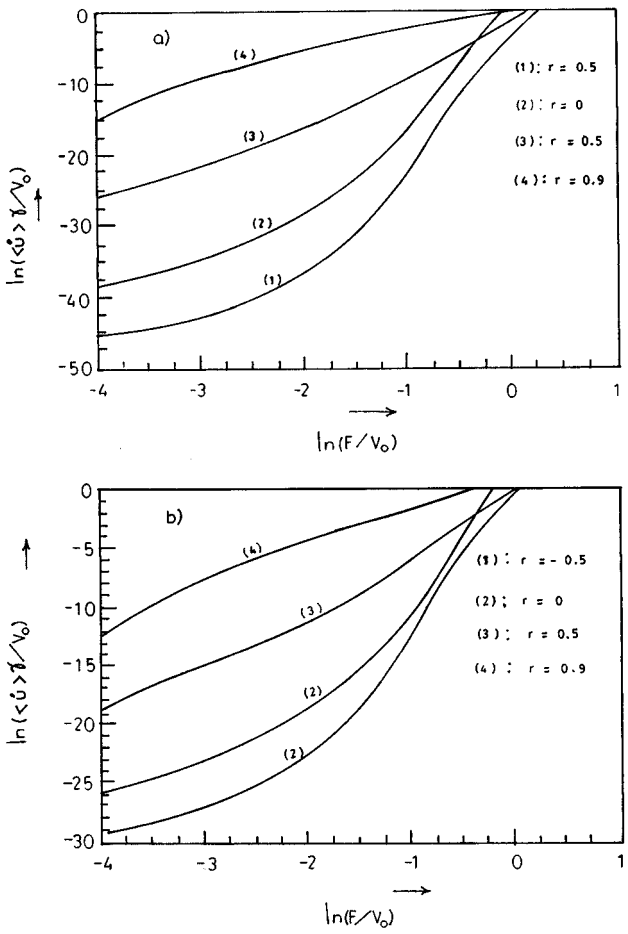

FIG. 10. Variation of average velocity of particles with F for a few values of shape parameter r with (a) $\tau = 0.2$, (b) $\tau = 0.3$, which increases F/V_0 for different shape parameter r.

charge [32]. Taking for the lattice parameters $a = 3$ Å, $D_s = 2.35$ eV, $\varepsilon_s = 0.11$ eV, $m = 1$ uma, $e^* = 0.5e$, and $r \simeq -0.3$, which is comparable to that existing in W and Ru, and $\gamma_0 = 6 \times 10^{13}$ s^{-1}, we obtain the following values of quantities:

$$V_0 \simeq 3.62 \times 10^{-2} \text{ eV Å}^{-1}, \quad \gamma = 7.62 \times 10^{-15} \text{ s}^{-1}, \quad \text{and}$$

$$k = 3.57 \times 10^{-1} \text{ eV Å}.$$

Here we have taken for the damping coefficient γ_0 the value which is equal to that of the proton migration in hydrogen-bonded solids [43,44].

Before analyzing the average displacement velocity of hydrogen atoms on Ru and W substrates, we first look at the motion of the driven kink in the electrical field E_e. As shown in Sec. II, E_e should be less than the critical field $E_c(r)$, which is an increasing function of r [see Fig. 1, where $E_e/E_C(r=0) = F/V_0$ with $E_c(r=0) = 2.35 \times 10^9$ V/m]. For the deformable parameter $r \simeq -0.3$, the critical electrical field has a value $E_c = 4.62 \times 10^9$ V/m. If the field E_e is very small ($E_e \ll E_c$), the driven kink velocity v is linear with respect to E_e. Hence, $v = \mu E_e$, where μ is a kink mobility. Figure 7 shows the variation of μ as a function of r, where the characteristic mobility μ_0 has a value μ_0

$=5.21\times10^{-2}$ cm^2 s^{-1} V^{-1}, corresponding to the characteristic diffusion coefficient $D_0=4.26\times10^{-4}$ cm^2 s^{-1} at $T=298$ K which follows from the modified Einstein relation $D=\mu k_BT/(2\pi e^*)$. For $r\simeq-0.3$, the diffusion coefficient has a value $D=3.4\times10^{-4}$ cm^2 s^{-1} comparable to that obtained in H/W and H/Ru adsystems since the experimental values show that D varies from 10^{-5} cm^2 s^{-1} to 10^{-3} cm^2 s^{-1} [40].

Also interesting in studying diffusion of hydrogen atoms on metallic surfaces is the mean displacement velocity of hydrogen atoms $\langle\partial\phi/\partial t\rangle$ induced by the electrical field. Note that $\langle\partial\phi/\partial t\rangle=(a/2\pi)\langle\partial u/\partial t\rangle$; this is given by Eq. (4.1). Our numerical applications are carried out for Ru and W substrates where we have taken the particular value $r\simeq-0.3$. The results are shown in Fig. 11 for three values of the temperature T. Theses figures show that $\langle\partial\phi/\partial t\rangle$ rises by several orders of magnitude in a small electrical field range around a particular value [see Fig. 11(a)], so that the threshold for energy localization could be reach. This suggests that the process of surface diffusion could be initiated by an energy-localization phenomenon, which is due to nonlinear effects. This evidences the importance of collective motion of adatoms (hydrogen atoms) observed at the time of experimental studies of surface diffusion [32].

VI. CONCLUSION

In this paper, we have studied the effect of a potential with variable shape on the nucleation rate of kink-antikink pairs in a one-dimensional chain following the Büttiker and Landauer theory [14]. The mean advantage of this potential lies in the fact that it can be used to describe a large amount of physical systems. As a result, an appropriate choice of the shape parameter r enables us to employ a suitable form of the shape close to the system under consideration such as epitaxial or incommensurate structure [32] in crystals and other various systems. The nucleation rate j_N has been obtained in the form $\Omega e^{-\Delta E_N(r,F)/k_BT}$, in agreement with the results of Ref. [45]. As in the SG case the prefactor Ω is proportional to $T^{-1/2}$ independent of the shape parameter r, however, it depends strongly on this parameter. Consequently, the nucleation rate of kink-antikink pairs not only depends on the external field, but also on the shape parameter r. This investigation is limited to the field $F\gg n_0k_BT$ where nucleation theory is valid. Here n_0 designates the (anti)kink mean density. At last, the velocity of the driven kink has been derived. As a consequence of the r dependence of the kink width [28], in response to an external field, the large kink ($r\to1$) moves more rapidly than the short one ($r\to-1$). This may be understood if we appeal to the fact that the short kink interacts with the particles of the chain, while the large kink does not see the particles [46,47].

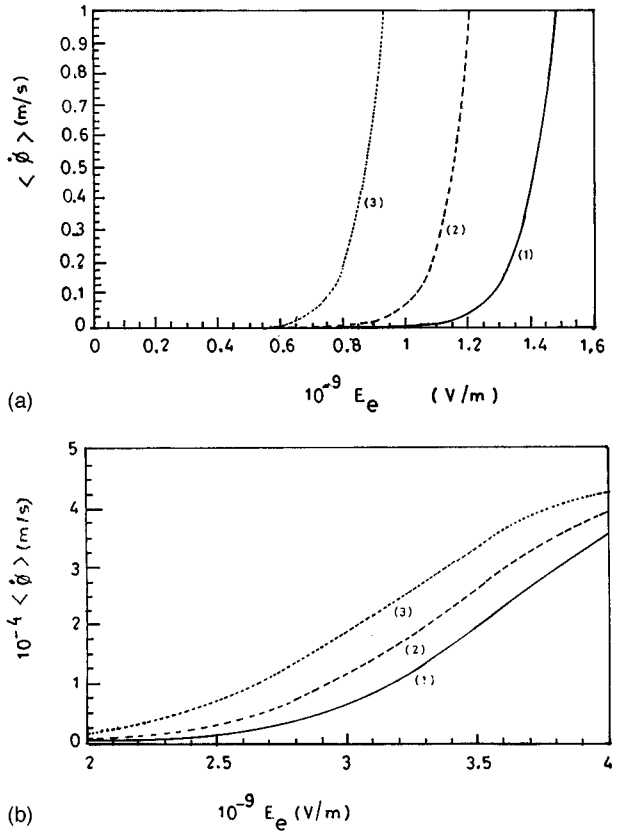

FIG. 11. Variation of $\langle\partial\phi/\partial t\rangle\equiv\langle\dot{\phi}\rangle$ (m/s) as a function of the electrical field for three values of the temperature; (1) $T=298$ K, (2) $T=393$ K, (3) $T=493$ K: (a) for small field ($E_e\ll E_c$), (b) for large field ($E_e\leqslant E_c$).

[1] H. Weiner, Phys. Rev. A **136**, 863 (1964).
[2] W. Atkinson and N. Cabrera, Phys. Rev. A **138**, 763 (1965).
[3] J. A. Krumhansl and J. R. Schrieffer, Phys. Rev. B **11**, 3535 (1975).
[4] T. Fonseca, J. A. N. F. Gomes, P. Grigolini, and F. Marchesoni, J. Chem. Phys. **80**, 1826 (1984).
[5] See review article by A. C. Scott, F. Y. F. Chu, and D. W. McLaughlin, Proc. IEEE **61**, 1443 (1973).
[6] M. B. Fogel, S. E. Trullinger, A. R. Bishop, and J. A. Krumhansl, Phys. Rev. B **15**, 1578 (1977).
[7] D. W. McLaughlin and A. C. Scott, Phys. Rev. A **18**, 1652 (1978).
[8] D. J. Kaup and O. El-Sayed, Phys. Rev. B **33**, 1762 (1986).
[9] Y. S. Kivshar and B. A. Malomed, Rev. Mod. Phys. **61**, 763 (1989).
[10] P. Woafo and T. C. Kofane, J. Phys. Condens. Matter **5**, 7063 (1993).
[11] P. Woafo and T. C. Kofane, Solid State Commun. **87**, 921 (1993).
[12] S. E. Trullinger, M. D. Miller, R. A. Guyer, A. R. Bishop, F. Palmer, and J. A. Krumhansl, Phys. Rev. Lett. **406** (1978).
[13] R. A. Guyer and M. D. Miller, Phys. Rev. A **17**, 1774 (1978).
[14] M. Büttiker and R. Landauer, Phys. Rev. A **23**, 1397 (1981).
[15] D. J. Scalapino, M. Sears, and R. A. Ferell, Phys. Rev. B **6**, 3409 (1972).
[16] H. C. Brinkman, Physica (Utrecht) **12**, 149 (1956).

[17] R. Landauer and J. A. Swanson, Phys. Rev. **121**, 1668 (1961).
[18] J. S. Langer, Phys. Rev. Lett. **21**, 973 (1968).
[19] S. N. Behera and A. Khare, J. Phys. Coll. **42**, C-6314 (1981).
[20] E. Magyari, Z. Phys. B **43**, 345 (1981).
[21] A. M. Dikande and T. C. Kofané, Phys. Lett. A **115**, 403 (1991).
[22] A. M. Dikande and T. C. Kofané, J. Phys. Condens. Matter **3**, 5203 (1991).
[23] T. C. Kofané and A. M. Dikande, Solid State Commun. **86**, 749 (1993).
[24] P. Tchofo Dinda, Phys. Rev. B **46**, 12 012 (1992).
[25] A. M. Dikande and T. C. Kofané, Solid State Commun. **89**, 283 (1994).
[26] A. M. Dikande and T. C. Kofané, Solid State Commun. **89**, 559 (1994).
[27] A. V. Zolotariuk and St. Pnevmatikos, Phys. Lett. A **143**, 233 (1990).
[28] M. Remoissenet and M. Peyrard, J. Phys. C **14**, L481 (1981).
[29] M. Peyrard and M. Remoissenet, Phys. Rev. B **26**, 2886 (1982).
[30] M. Remoissenet and M. Peyrard, Phys. Rev. B **29**, 3153 (1984).
[31] S. De Lillo and P. Sodano, Lett. Nuovo Cimento **37**, 380 (1983).
[32] O. M. Braun, Yu. S. Kivshar, and I. I. Zelenskaya, Phys. Rev. B **41**, 7118 (1990), and references therein.
[33] M. Croitoru, J. Phys. A **20**, 1695 (1987).
[34] Masatoshi Imada, J. Phys. Soc. Jpn. **52**, 1946 (1983).
[35] A. Kenfack and T. C. Kofané (unpublished).
[36] D. L. Landau and E. M. Lifshitz, *Quantum Mechanics* (Addison-Wesley, Reading, MA, 1968).
[37] A. Seeger, Philos. Mag. **1**, 651 (1956); J. Lothe and J. P. Hirth, Phys. Rev. **115**, 543 (1959).
[38] R. Landauer, Phys. Rev. A **15**, 2117 (1977).
[39] M. Büttiker and H. Thomas, Phys. Rev. A **37**, 235 (1988).
[40] R. Gomer, Rep. Prog. Phys. **53**, 917 (1990).
[41] R. Gomer and J. K. Hulm, J. Chem. Phys. **27**, 1363 (1957); C. Dharmadhikari and R. Gomer, Surf. Sci. **143**, 223 (1984).
[42] C. H. Mak, J. L. Brand, A. A. Deckert, and S. M. George, J. Chem. Phys. **85**, 1676 (1986).
[43] P. Woafo, R. Takontchoup, and A. S. Bokosah, J. Chem. Phys. Solids **56**, 1277 (1995).
[44] S. Yomosa, Phys. Rev. A **32**, 1752 (1985); D. Hochstrasser, F. G. Mertens, and H. Büttner, Phys. Rev. A **40**, 2602 (1989).
[45] M. Büttiker, E. P. Harris, and R. Landauer, Phys. Rev. B **28**, 1268 (1983).
[46] P. Woafo, T. C. Kofané, and A. S. Bokosah, J. Phys. Condens. Matter **3**, 2279 (1991).
[47] P. Woafo, T. C. Kofané, and A. S. Bokosah, J. Phys. Condens. Matter **4**, 3389 (1992).